Supplement of Atmos. Meas. Tech., 8, 1–18, 2015
http://www.atmos-meas-tech.net/8/1/2015/
doi:10.5194/amt-8-1-2015-supplement
© Author(s) 2015. CC Attribution 3.0 License.

Atmospheric Measurement Techniques
Open Access

Supplement of

Application of high-resolution time-of-flight chemical ionization mass spectrometry measurements to estimate volatility distributions of α-pinene and naphthalene oxidation products

P. S. Chhabra et al.

Correspondence to: P. S. Chhabra (pschhabra@utexas.edu)

1 Average Relative Sensitivity

An average sensitivity factor was applied for species detected by the acetate-CIMS based upon literature data from Veres et al. (2010); Yatavelli et al. (2012); Aljawhary et al. (2013). Sensitivities measured for various acids normalized to the formic acid sensitivity are compiled in Supplemental Table 1. The average relative acetate-CIMS sensitivity, 1.3 ± 0.8, is multiplied to the measured 5.5 ± 0.9 Hzppt^{-1} sensitivity of formic acid. Thus, to all acid signals (except formic), we apply a total sensitivity of 7.1 ± 4.6 Hzppt^{-1}.

Supp. Table 1. Relative sensitivities of various organic acids and their corresponding references. Since pyruvic acid appears twice, the average is used the in the determination of the average relative acetate-CIMS sensitivity.

Organic Acid	Relative Sensitivity to Formic Acid	Reference
succinic acid	2.20119	Aljawhary et al. (2013)
malonic acid	2.09693	Aljawhary et al. (2013)
glyoxylic acid	1.861	Aljawhary et al. (2013)
oxalic acid	1.24072	Aljawhary et al. (2013)
pyruvic acid	1.39841	Aljawhary et al. (2013)
tartaric acid	0.892451	Aljawhary et al. (2013)
citric acid	0.53865	Aljawhary et al. (2013)
pinonic acid	1.76795	Aljawhary et al. (2013)
pyruvic acid	1.45291	Veres et al. (2010)
glycolic acid	1.79056	Veres et al. (2010)
methacrylic acid	0.233644	Veres et al. (2010)
acrylic acid	0.695613	Veres et al. (2010)
propionic acid	0.0348808	Veres et al. (2010)
palmitic acid	0.54	Yatavelli et al. (2012)
azelaic acid	0.88	Yatavelli et al. (2012)
tricarballyic acid	2.6	Yatavelli et al. (2012)

2 Estimation of Uncertainty in Vapor Pressures and Partitioning

We derive a correlation of uncertainty as a function of vapor pressure from Figure 12 of Pankow and Asher (2008), reproduced here as Supplemental Figure 1. The parameter σ_{FIT} represents the average of the absolute

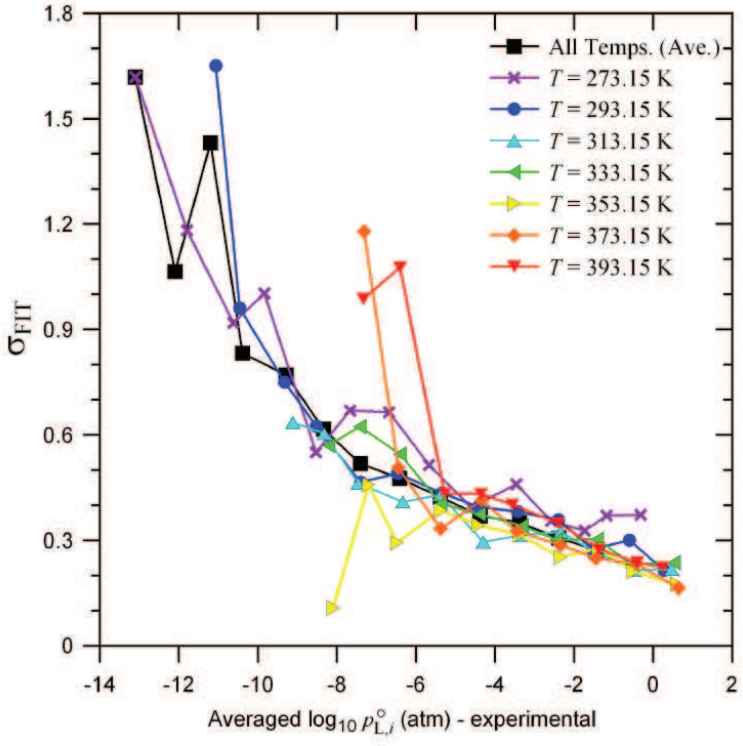

Supp. Fig. 1. Figure 12 reproduced from Pankow and Asher (2008) illustrating decadally binned averages of σ_{FIT} as a function of the log of experimental vapor pressure.

deviations between the logarithm of predicted and experimental pressures, decadally binned according to the log of the experimental vapor pressure:

$$\sigma_{FIT} = \frac{1}{N}\sum_{i=1}^{N_C}\sum_{j=1}^{N_{T,i}}\left|\log_{10}\left(p^0_{L,i}(T_{j,i})_P\right) - \log_{10}\left(p^0_{L,i}(T_{j,i})_E\right)\right| \quad (1)$$

To estimate σ_{FIT} as a function of vapor pressure, data from Response Figure 1 from temperatures 273.15 to 333.15K were extracted and fitted with an exponential function (σ_{CORR}) as shown in Response Figure 2, where:

$$\sigma_{CORR} = y_0 + Ae^{\left(\frac{-(p^0_{L,i}-x_0)}{\tau}\right)} \quad (2)$$

The average absolute deviation from the mean is less than or equal to the standard deviation, and for a normal distribution the ratio of the mean absolute deviation to the standard deviation is $\sqrt{2/\pi}$ (Geary, 1935). Thus,

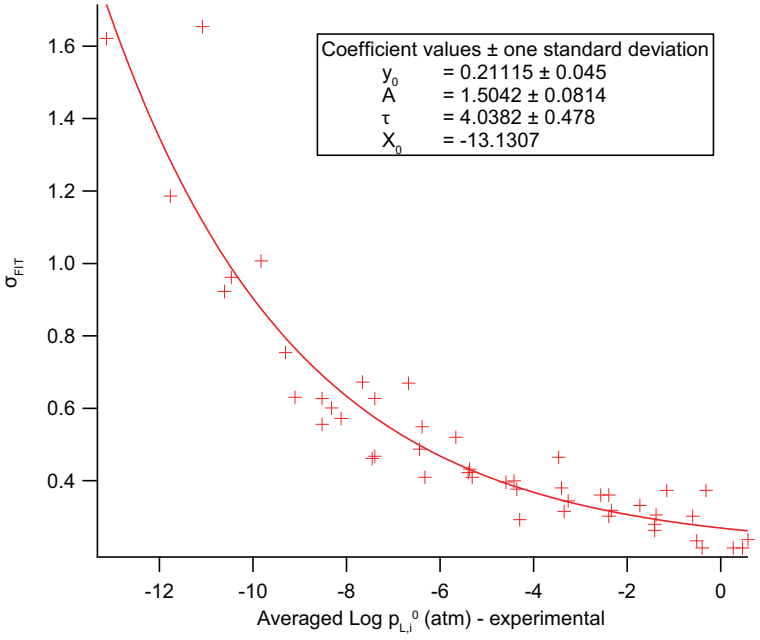

Supp. Fig. 2. Exponential correlation between σ_{FIT} and average log of vapor pressure binned to the nearest integer

to provide a more conservative estimate of the error, we divide σ_{CORR} by $\sqrt{2/\pi}$:

$$\sigma_{SIM} = \frac{y_0 + Ae^{\left(\frac{-(p^0_{L,i} - x_0)}{\tau}\right)}}{\sqrt{2/\pi}} \tag{3}$$

where σ_{SIM} represents the uncertainty in SIMPOL vapor pressure (in $\log(\mathrm{atm})$) used in our analysis. σ_{SIM} is propagated through the analysis and from which uncertainties in c^* and ξ_i are calculated using standard error propagation rules. Because $\log_{10}(p^0_{L,i})$ and $\log_{10}(c^*_i)$ differ by a constant,

$$\sigma_{\log_{10} c^*_i} = \sigma_{SIM} \tag{4}$$

Thus:

$$\sigma_{c^*_i} = \left|10^{\log_{10} c^*_i}\right| \sigma_{\log_{10} c^*_i} (\ln 10) \tag{5}$$

and

$$\sigma_{\xi_i} = \frac{\sigma_{c^*_i}}{C_{OA}\left(1 + \frac{c^*_i}{C_{OA}}\right)^2} \tag{6}$$

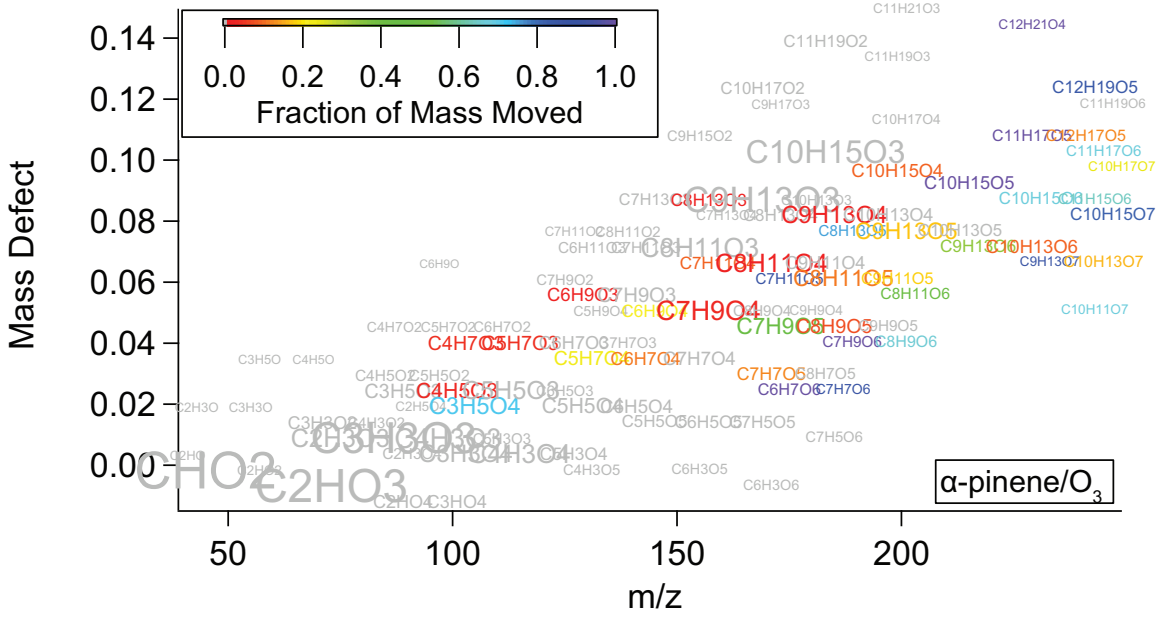

Supp. Fig. 3. Mass defect plot of α-ozonolysis CIMS spectra (Expt. 1). The text of each marker represents the chemical formula of the identified CIMS anion. The size of each marker represents the mass fraction of that ion in the spectra. The color of each ion is scaled to indicate how much of its signal is subtracted and given to its base ion (molecular formula less $C_2H_4O_2$). A gray color indicates less than 1% of the signal is moved.

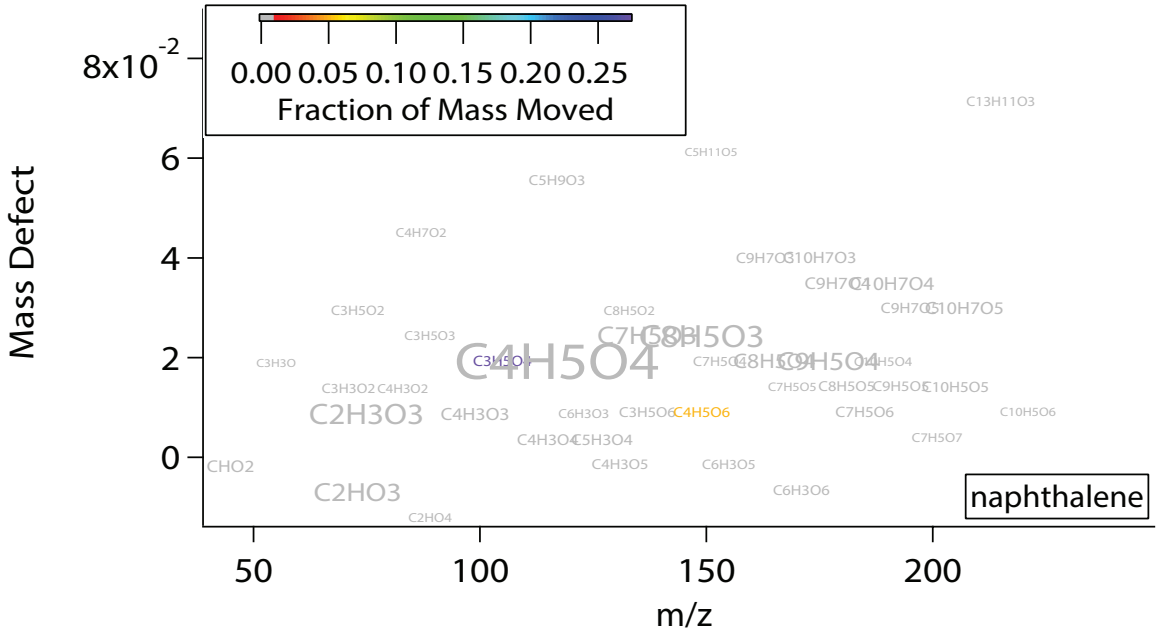

Supp. Fig. 4. Mass defect plot of naphthalene photooxidation CIMS spectra (Expt. 12). The text of each marker represents the chemical formula of the identified CIMS anion. The size of each marker represents the mass fraction of that ion in the spectra. The color of each ion is scaled to indicate how much of its signal is subtracted and given to its base ion (chemical formula less $C_2H_4O_2$). A gray color indicates less than 1% of the signal is moved.

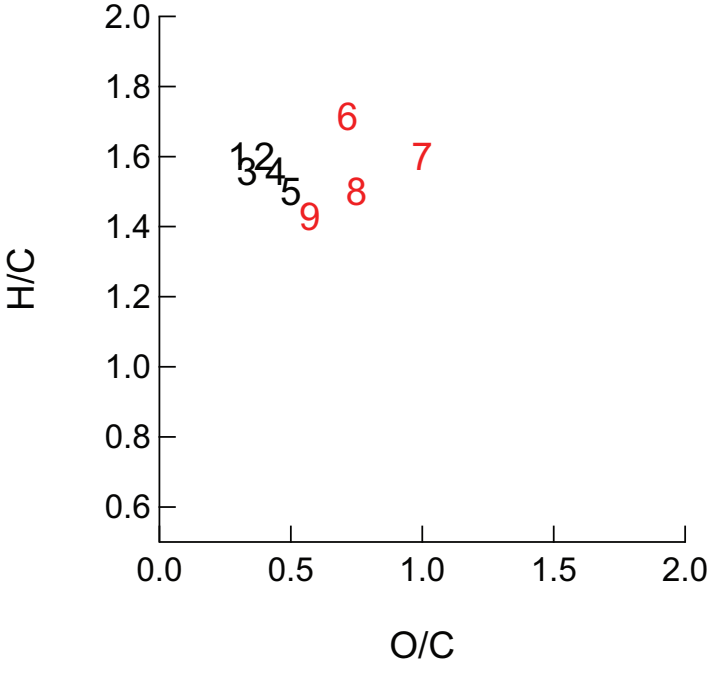

1. pinonic acid
2. hydroxy pinonic acid
3. norpinonic acid
4. pinic acid
5. norpinic acid
6. 3-hydroxy-2,2-dimethylglutaric acid
7. 3-hydroxyglutaric acid
8. 3-methyl-1,2,3-butanetricarboxylic acid
9. terebic acid

Supp. Fig. 5. Van Krevelen plot of tracer acids from the α-pinene system, as shown in Figure 3, Panel A. Tracers are numbered, corresponding to their proposed identities shown below. Tracers identified by Yu et al. (1999) are in black and tracers identified by Claeys et al. (2013) are in red.

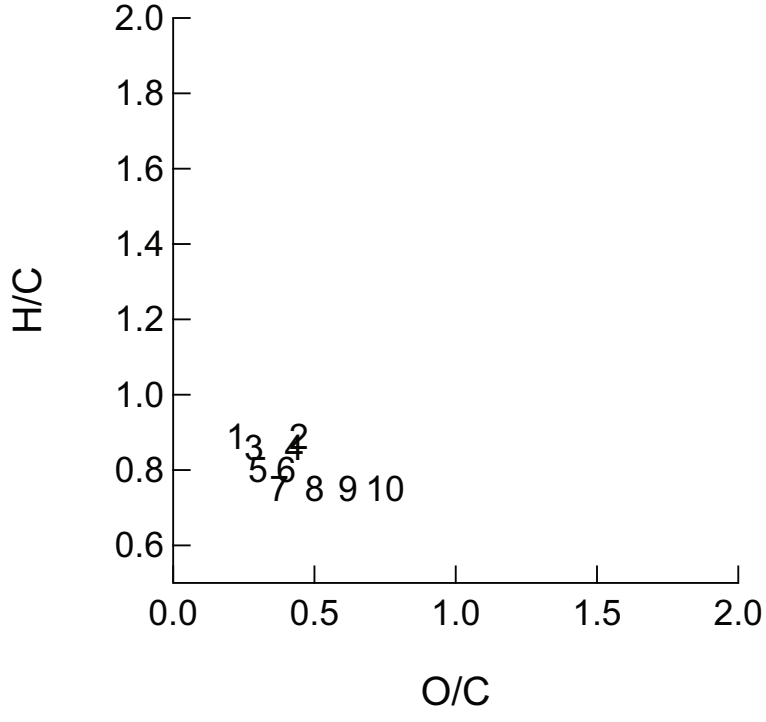

1. cinnamic acid
2. dihydroxy cinnamic acid
3. benzoic acid
4. hydroxy benzoic acid
5. formyl cinnamic acid
6. carboxycinnamic acid
7. phthaldehydic acid
8. phthalic acid
9. hydroxy phthalic acid
10. dihydroxy phthalic acid

Supp. Fig. 6. Van Krevelen plot of tracer acids from the naphthalene system, as shown in Figure 3, Panel B (Kautzman et al., 2009). Tracers are numbered, corresponding to their proposed identities shown below.

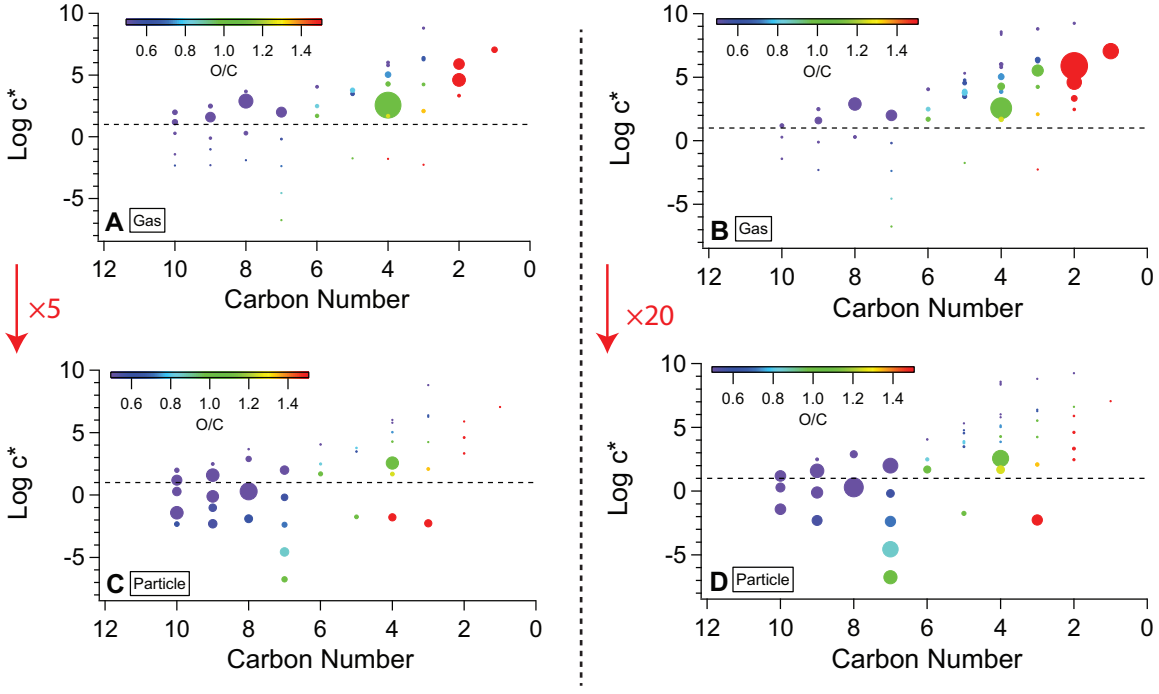

Supp. Fig. 7. Estimated Log c* as a function of carbon number and O/C for two different naphthalene photooxidation experiments. Panels A and C represent extracted gas and particle spectra of Expt. 12 respectively, and Panels B and D represent the same of Expt. 15. Marker size is proportional to the fraction of mass. The factor and arrow in red represents the relative mass scale between gas and particle spectra. For example ×20 between panels B and D indicate that markers of equal area represent equal fractions in their respective phases and 20 times more mass in the gas-phase spectrum.

References

Aljawhary, D., Lee, A. K. Y., and Abbatt, J. P. D.: High-resolution chemical ionization mass spectrometry (ToF-CIMS): application to study SOA composition and processing, Atmos. Meas. Tech., 6, 3211–3224, doi:10.5194/amt-6-3211-2013, aMT, 2013.

Claeys, M., Szmigielski, R., Vermeylen, R., Wang, W., Shalamzari, M., and Maenhaut, W.: Tracers for Biogenic Secondary Organic Aerosol from alpha-Pinene and Related Monoterpenes: An Overview, book section 18, pp. 227–238, NATO Science for Peace and Security Series C: Environmental Security, Springer Netherlands, doi:10.1007/978-94-007-5034-0_18, 2013.

Geary, R. C.: The Ratio of the Mean Deviation to the Standard Deviation as a Test of Normality, Biometrika, 27, 310–332, doi:10.2307/2332693, 1935.

Kautzman, K. E., Surratt, J. D., Chan, M. N., Chan, A. W. H., Hersey, S. P., Chhabra, P. S., Dalleska, N. F., Wennberg, P. O., Flagan, R. C., and Seinfeld, J. H.: Chemical Composition of Gas- and Aerosol-Phase Products from the Photooxidation of Naphthalene, The Journal of Physical Chemistry A, 114, 913–934, doi:10.1021/jp908530s, 2009.

Pankow, J. F. and Asher, W. E.: SIMPOL.1: a simple group contribution method for predicting vapor pressures and enthalpies of vaporization of multifunctional organic compounds, Atmos. Chem. Phys., 8, 2773–2796, doi:10.5194/acp-8-2773-2008, aCP, 2008.

Veres, P., Roberts, J. M., Burling, I. R., Warneke, C., de Gouw, J., and Yokelson, R. J.: Measurements of gas-phase inorganic and organic acids from biomass fires by negative-ion proton-transfer chemical-ionization mass spectrometry, Journal of Geophysical Research: Atmospheres, 115, D23 302, doi:10.1029/2010JD014033, 2010.

Yatavelli, R. L. N., Lopez-Hilfiker, F., Wargo, J. D., Kimmel, J. R., Cubison, M. J., Bertram, T. H., Jimenez, J. L., Gonin, M., Worsnop, D. R., and Thornton, J. A.: A Chemical Ionization High-Resolution Time-of-Flight Mass Spectrometer Coupled to a Micro Orifice Volatilization Impactor (MOVI-HRToF-CIMS) for Analysis of Gas and Particle-Phase Organic Species, Aerosol Science and Technology, 46, 1313–1327, doi:10.1080/02786826.2012.712236, 2012.

Yu, J., Cocker, DavidR, I., Griffin, R., Flagan, R., and Seinfeld, J.: Gas-Phase Ozone Oxidation of Monoterpenes: Gaseous and Particulate Products, Journal of Atmospheric Chemistry, 34, 207–258, doi:10.1023/A:1006254930583, 1999.